Eur. Phys. J. B **14**, 337–348 (2000)

THE EUROPEAN PHYSICAL JOURNAL B

EDP Sciences

Confined electron and shallow donor states in graded $GaAs/Al_xGa_{1-x}As$ spherical quantum dots

Jian-Min Shi, V.N. Freire[a], and G.A. Farias

Departamento de Física, Universidade Federal do Ceará, C.P. 6030, Campus do Pici, 60455-760 Fortaleza, Ceará, Brazil

Received 31 May 1999

Abstract. A theoretical study is performed on the confined electron and shallow donor states properties in graded $GaAs/Al_xGa_{1-x}As$ spherical quantum dots. The two lowest energy levels of a confined electron are obtained taking into account the dependence of the electron effective mass on the spatial profile of the Al molar fraction. The ground state of a single Si shallow donor, which may be located at an arbitrary position in the structure, is calculated through a variational approach. Depending on the dot interface width and localization, we find that the energy levels of the electron and donor states for the system under study can be blue or red shifted appreciably in comparison to those calculated within the sharp interface picture. We show that it is necessary to have accurate information concerning the interface of semiconductor dots whose samples are used in the experiments, in order to achieve a better understanding of their optical properties.

PACS. 68.10.Gw Interface activity, spreading – 68.65.+g Low-dimensional structures (superlattices, quantum well structures, multilayers): structure, and nonelectronic properties – 71.23.An Theories and models; localized states

1 Introduction

Due to advances in modern crystal-growth techniques such as molecular-beam epitaxy and metalorganic chemical vapor deposition, the investigation of confined electron as well as impurity (donor or acceptor) states in low-dimensional structures such as quantum wells (QWs), superlattices, quantum wires, and quantum dots (QDs) has attracted a lot of theoretical and experimental attention during the last two decades [1–6]. Recently one has been able to grow semiconductor QDs in macroscopic quantities with a high degree of control and reproducibility [7] to investigate three-dimensional (3D) carriers confinement, both for fundamental study in physics and for possible device applications in the case of the particularly sharp state density [8]. This progress has motivated many experimental studies on the electronic and optical properties of the zero-dimensional (0D) electron systems [9]. One of the most interesting phenomena is the effect of dot-size fluctuations on the energy levels in such strong confinement structures [10–12]. Since the optical and transport properties in bulk and low-dimensional semiconductors are strongly influenced by the electron localization, impurity energy levels, and also by the types of low-dimensional structures, the knowledge of the confinement potential effect on the electron states is essential [13,14].

In a single (or isolated) QD, the energy spectrum of electrons is completely discrete and has atomic-like energy levels. Therefore, the electrons localized in this quasi-zero-dimensional system have some common features with shallow donors in semiconductors. For small-size dots with high barriers, the confinement energy is much stronger than the Coulomb interaction. As a consequence, one is allowed to use the nearly independent particle limit to describe the electron states in these structures [15]. Recently, experiments involving an ensemble of QDs have revealed a difference when compared to epitaxially grown quantum dots, *i.e.,* the transition linewidths in the former are significantly broader than those in the later [16–19]. The reason for this difference has been supposed to be due to dot-size fluctuation effects.

Most of the previous theoretical analysis on the electron states in semiconductor QDs (in particular, $GaAs/Al_xGa_{1-x}As$ QDs) addressed sharp confinement models, *i.e.,* the interface is considered to be absolutely sharp so that the confinement potential can be expressed by a 3D square-well, for example. However, experimental results have shown that the interfaces between GaAs and $Al_xGa_{1-x}As$ are not abrupt, and they extend through a region at least as wide as two GaAs unit cells along the growth axis of their two dimensional confinement structures [20]. The same should occur for heterostructures with other types of semiconductors. While considerable effort was developed for the understanding of interface

[a] valder@fisica.ufc.br

effects in 2D semiconductor confinement systems [21,22], this is not the case for semiconductor QDs. Recently, we have found in two preliminary investigations that the effect of a graded interface is more pronounced for an electron as well as a shallow donor in a QD than in a QW due to the stronger confinement [23,24]. However, in those two previous theoretical works we have considered only the case of the interface inside the well (dot) material, which always enhances the confinement effect of the system, and consequently leads to a blue shift of the electron energy levels.

The aim of this work is to develop a systematic investigation of interface related effects on the energy levels of an electron and a Coulomb-bound electron in a QD structure, in particular taking into account the interface localization. Consequently, it is essential to consider not only the interface width but also to specify all their possible locations in the structure, and how to describe the role of both (width and location) on the QDs confinement properties. Two parameters describing the interface are introduced, the interface width W and the interface localization α, which span a special two-dimensional (2D) space in such a way that we can easily discuss the electron energy shift due to the interface effect.

This paper is organized as follows. In Section 2, we describe the interface and shallow donor model, as well as our theoretical approach to solve the Schrödinger-like equations for an electron in a graded GaAs/Al_xGa_{1-x}As spherical QD in the absence and in the presence of a Si-donor ion within the multistep approach. In Section 3, the numerical results are presented describing the electron states, their energy levels and their intersubband ($1s \rightarrow 2p$) transition energies, which are analyzed in the $W-\alpha$ space. A similar procedure is undertaken in Section 4 for the energy level and the binding energy of the shallow donor ground state. Section 5 is devoted to our discussions and conclusions.

2 Interface description and calculation approach

The quantum dot we consider consists of a GaAs sphere of radius R immersed in a $Al_xGa_{1-x}As$ bulk alloy. The GaAs dot is surrounded by a cap, which is a graded interface with finite width W, extending from $R-\alpha W$ to $R+(1-\alpha)W$, as shown in Figure 1. In doing so, we have chosen the dot center as the origin of our coordinates. A variation of two interface parameters, W and α, can represent the dot-size fluctuation in the structures: a change in the interface width (W) corresponds to a barrier positioning fluctuation, while a variation in the interface position (α) to a dot-radius fluctuation. In experiments, the interface width can be measured accurately, and shows a typical value at least of two GaAs lattice constants [20,25]. Since the parameter α is introduced to indicate the interface location, it is natural that $0 \geq \alpha \geq 1$. When $\alpha = 0.5$, the sharp barrier is located at the middle of the interface, while for $\alpha = 1$ ($\alpha = 0$) the interface region is restricted to be completely inside (outside) the reference QD square well region.

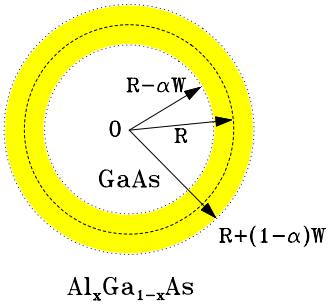

Fig. 1. Diagram of a graded GaAs/$Al_xGa_{1-x}As$ spherical quantum dot. R is the dot radius, W is the interface width, and $\alpha = (0,\ 1)$ determines the interface position.

Within the framework of the standard effective-mass approximation [26], the Hamiltonian describing an electron state in the GaAs/$Al_xGa_{1-x}As$ QD structure can be written as

$$H = -\frac{\hbar^2}{2}\nabla\frac{1}{m^*(r)}\nabla - \frac{Z_D e^2}{\epsilon_0|r-R_0|} + V(r), \qquad (1)$$

where r is the position of the electron, the second term corresponds to the Coulomb interaction; Z_D is the donor ions number with charge $+e$; $Z_D = 0$ for a free electron, and $Z_D = 1$ for a Si donor located at position R_0; $\epsilon_0 = 12.5$ is the GaAs dielectric constant [27], which is assumed to be uniform in the whole structure, and the last term is the QD confinement potential.

In equation (1), the graded spherical QD confinement potential $V(r)$ depends on the interfacial aluminum molar fraction in the structure, and is modeled by the following expression [28]

$$V(r) = \begin{cases} 0, & r < R-\alpha W; \\ 0.693y + 0.222y^2\ (\text{eV}), & R-\alpha W < r < R+(1-\alpha)W; \\ 0.693x + 0.222x^2\ (\text{eV}), & r > R+(1-\alpha)W, \end{cases} \qquad (2)$$

where $y(r)$ describes the interfacial Al molar fraction profile, which is assumed to be given by

$$y(r) = x\left[\frac{r+\alpha W-R}{W}\right]. \qquad (3)$$

In equation (2), the electron band offset is considered to be 60% of the total band-gap difference between GaAs and $Al_xGa_{1-x}As$ [29]. $m^*(r)$ is the electron effective mass, which also depends on the interfacial profile of the Al molar fraction, and is given by the formula [27]

$$m^*(r)/m_e = \begin{cases} 0.067, & r < R-\alpha W; \\ 0.067 + 0.083y, & R-\alpha W < r < R+(1-\alpha)W; \\ 0.067 + 0.083x, & r > R+(1-\alpha)W, \end{cases} \qquad (4)$$

where m_e is the electron mass in vacuum. This type of linear dependence was used in previous works for different systems [23,24], but limiting the interface to be totally inside wells or dots (*i.e.*, $\alpha = 1$), so that it always was found to increase the confinement effect.

Since the interface effect on the electron state becomes experimentally negligible in weakly confined systems, we will limit ourselves mainly to strong confinement QDs. The spherical polar coordinates have been taken for the study of the free electron states, while the cylindrical polar coordinates was used for the shallow donor state description, where the donor center is fixed on the z axis at $R_0 = (0, 0, R_0)$. In this work, the Al molar fraction in the bulk $Al_xGa_{1-x}As$ alloy for $r > R + (1-\alpha)W$ has been fixed as $x = 0.3$. For our convenience, we remember that for GaAs the effective Bohr radius is $a_0^* = \hbar^2\epsilon_0/m^*(0)e^2 = 98.7$ Å, and the effective Rydberg is $R^* = e^2/2\epsilon_0 a_0^* = 5.83$ meV.

By disregarding the electron-electron interaction, the Schrödinger equations can be solved exactly for a spherical sharp (abrupt) QD confined electron and also for an electron bound to a shallow donor confined in a sharp spherical QD (*i.e.*, $W = 0$) when the electron mass is considered to be uniform in the whole structure [4,30]. However, until now it is still impossible to obtain an analytical solution when the existence of a graded (nonabrupt) interface is considered, as a consequence of the spatial dependence of the electron effective mass. Therefore, we rely on a multistep approach [31] to solve the Schrödinger equation with the Hamiltonian H since it can not be solved analytically in our structures. The interface is divided into N segments, and the Al concentration is taken as a constant in each of them. Thus, the continuous interface potential is replaced by a multistep potential well. Its continuous change can be recovered provided that the segments become finer and finer (*i.e.*, $N \to \infty$). Therefore, equations (2) and (4) for the confinement potential and the electron effective mass in the interface region are approximated, respectively, by the multistep functions

$$V(r) \to V_j = V\left(\frac{r_{j-1} + r_j}{2}\right), \tag{5}$$

and

$$m^*(r) \to m_j^* = m^*\left(\frac{r_{j-1} + r_j}{2}\right), \tag{6}$$

for $r_{j-1} < r < r_j$ with $j = 0, 1, 2, \cdots, N, N+1$. Notice that $j = 0$ corresponds to the $y = 0$ region where $V(r) = 0$, and $j = N + 1$ to the $y = x$ region in which $V(r) = V_{\mathrm{MAX}} = 0.693x + 0.222x^2$ eV. In this work, only the ground ($1s$-like) state and the lowest excited ($2p$-like) state of a free electron will be studied, which have been shown to be the most important ones in the structures under investigation [4,23]. Although we have used the notation of the hydrogen-atom states for indicating the free electron states in a spherical QD, these states have quite different properties from each other due to the different types of confinement potentials [15].

In a spherically symmetric potential such as the spherical QD or the Coulomb potential, the wave functions of an electron have the well-defined orbital and magnetic quantum numbers. In the absence of any impurities [30] and does not taking care of the angular part $Y(\theta, \phi)$ (spherical harmonics) of the electron probability distribution, the radial part of the wave function $\psi_{\mu,j}(r)$, ($\mu = 1s$ and $2p$) of an electron in the μ-th state with energy E_μ and momentum $k_{\mu,j} = [2m_j^*(E_\mu - V_j)/m_e]^{1/2}/\hbar$ in the j-th region of the structure can be written in the following form

$$\psi_{1s} \to \psi_{1s,j}(r) = \frac{1}{r}[A_{1s,j}\exp(\mathrm{i}k_{1s,j}r) + B_{1s,j}\exp(-\mathrm{i}k_{1s,j}r)] \tag{7}$$

for the $1s$-like state with angular momentum quantum number $l = 0$, and

$$\psi_{2p} \to \psi_{2p,j}(r) = A_{2p,j}\frac{1}{r}\left(1 + \frac{1}{k_{2p,j}r}\right)\exp(\mathrm{i}k_{2p,j}r) + B_{2p,j}\frac{1}{r}\left(1 - \frac{1}{k_{2p,j}r}\right)\exp(-\mathrm{i}k_{2p,j}r) \tag{8}$$

for the $2p$-like state with $l = 1$. Considering the current-conserving conditions for both $\psi_{\mu,j}(r)$ and $(1/m_j^*)(\mathrm{d}\psi_{\mu,j}/\mathrm{d}r)$ at each boundary of all the steps, the wave function normalization, and using the fact that $\psi_{\mu,j}(r) \to 0$ when $r \to \infty$, one can determine all the coefficients $A_{\mu,j}$, $B_{\mu,j}$ and the energy E_μ of the μ-th state by solving numerically a matrix equation resulting from a multiplication of $N + 1$ (2×2) transfer matrixes equation [31].

For the structure with a donor at position $R_0 \neq 0$, the spherical symmetry of the system is broken. Therefore, an exact solution for the Schrödinger equations becomes impossible even in the case of the uniform electron effective mass [4]. A variational calculation for the ground state (also called $1s$-like) of the electron is developed using a similar scheme for donors in QWs and superlattices [3]. Since in general the electron energy related to the QD potential is much larger than the Coulomb energy, one can explicitly factor out the associated lowest-energy solution of a free electron from the wave function of the donor state [32,33]. Consequently, the radial part of the variational wave function of the electron ground state can be expressed as a product of two functions,

$$\Psi_{1s}(r, R_0) = \psi_{1s}(r)\exp\left[-\beta\sqrt{\rho^2 + \gamma^2(z - R_0)^2}\right], \tag{9}$$

where the donor position has been chosen at $R_0 = |(0, 0, R_0)|$; ρ is the electron distance in the x-y plane. The first factor on the right-hand side of equation (9) is the wave function of the free electron ground state given by equation (7), and the second is related to the Coulomb interaction between the electron ($-e$) and the donor ion ($+e$). The energy expectation value E_D of the electron state Ψ_{1s} is given by

$$E_D = \frac{\langle\Psi_{1s}(r, R_0)|H|\Psi_{1s}(r, R_0)\rangle}{\langle\Psi_{1s}(r, R_0)|\Psi_{1s}(r, R_0)\rangle} \tag{10}$$

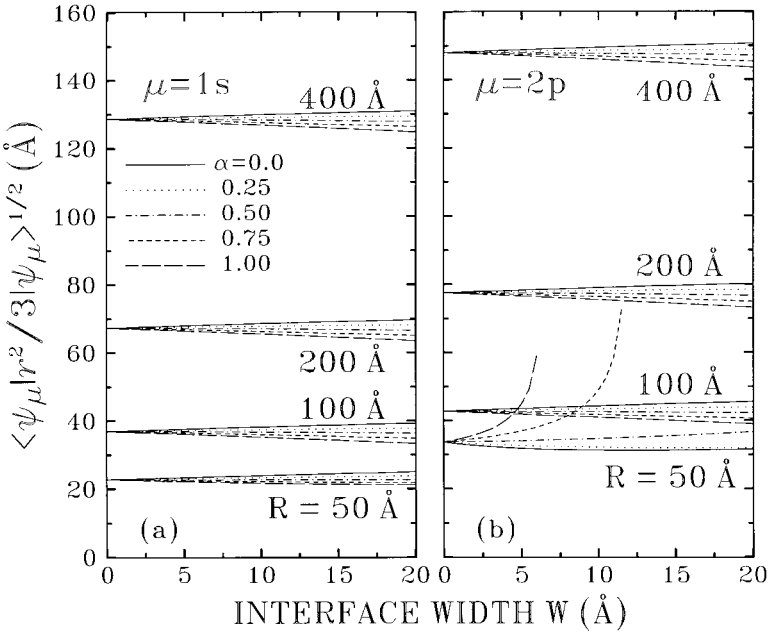

Fig. 2. The $1s$ (a) and $2p$ (b) state widths as a function of the interface width for an electron in $GaAs/Al_{0.3}Ga_{0.7}As$ quantum dots of radii $R = 50$ Å, 100 Å, 200 Å, and 400 Å. The interface positions are determined by different values of α: $\alpha = 0.00$ (solid), $\alpha = 0.25$ (dotted), $\alpha = 0.50$ (dashed dotted), $\alpha = 0.75$ (dashed), and $\alpha = 1.00$ (long dashed).

which can be minimized numerically through the two variational parameters β and γ. We have examined the accuracy of this approach. In both asymptotic limits of the QD size ($R \to \infty$ and $R \to 0$), the correct 3D hydrogenic behavior can be recovered. On the other hand, the difference between the present result and the exact solution obtained in reference [4] (defined as the binding energy E_B), which is given by

$$E_B = E_{1s} - E_D, \tag{11}$$

is very small, less than one percent for a donor located at the center of an abrupt $GaAs/Al_{0.3}Ga_{0.7}As$ QD with $R = 50$ Å.

3 The confined electron states

The effective mass approximation is applicable only for weakly bound states. In general, it requires an average radius larger than 20 Å for a confined electron in most semiconductors [26]. The effective Bohr radius of an electron bound to a shallow donor in bulk GaAs is about $a_0^* = 98.7$ Å. However, the average radius of the electron in GaAs-based low-dimensional structures should be much smaller than a_0^* when the confinement potential becomes stronger. In order to verify whether this approximation may be still suitable to strong confinement QDs, we plot in Figures 2a and 2b, respectively, the width of the $1s$ and $2p$ free electron states $\langle\psi_\mu|r^2/3|\psi_\mu\rangle^{1/2}$ as a function of the interface width up to 20 Å with $\alpha = 0.00$ (solid), 0.25 (dotted), 0.50 (dash-dotted), 0.75 (short-dashed), and 1.00 (long-dashed curves). Four different QDs with radii $R = 50$ Å (the lowest), 100 Å (second lowest), 200 Å (second highest), and 400 Å (highest groups) are considered. It is clearly shown that the QD potential confines the electron wave function considerably, and this confinement effect is strong when the dot size decreases. The width of the $1s$ state in an $R = 50$ Å QD with a 20 Å graded interface still has a value larger than 20 Å when $\alpha = 1.0$. As a consequence, the standard effective mass approximation is reliable for the present study. The difference between the $1s$ and $2p$ states shows that the influence of the potential confinement is not the same for each of them. In strong confinement dots, the relative state width difference between them are quite large, but becomes smaller very fast when the dot size increases since all of the states will degenerate for the case of a infinitely large dot. For example, the ratio between the $2p$-state and the $1s$-state widths is 1.48 for an abrupt QD with $R = 50$ Å, and then becomes 1.23, 1.16, and 1.15 for $R = 60$ Å, 100 Å and 200 Å, respectively.

The interface effect on the state width depends not only on the interface width itself, but also on the interface position, such that the interface width influences the absolute value of the state width, while its position determine if the state width increases or decreases. It is interesting to observe that the $2p$ state width for the $R = 50$ Å dot increases dramatically for the highest α (for which the part of the interface located inside the dot is stronger) when the interface width becomes wider. Our results are consistent with the exact ones: there are no bound states for an abrupt QD with radius $R < R_{MIN} = \pi\hbar/(8m^*V_{MAX})^{1/2}$, and no excited states when $R < 2R_{MIN}$ [30] in the case of the uniform electron effective mass. This is different from the electronic subbands case in 2D structures, in which the lowest subband is always bound. We will show later that when the dot radius decreases further, the $1s$ state

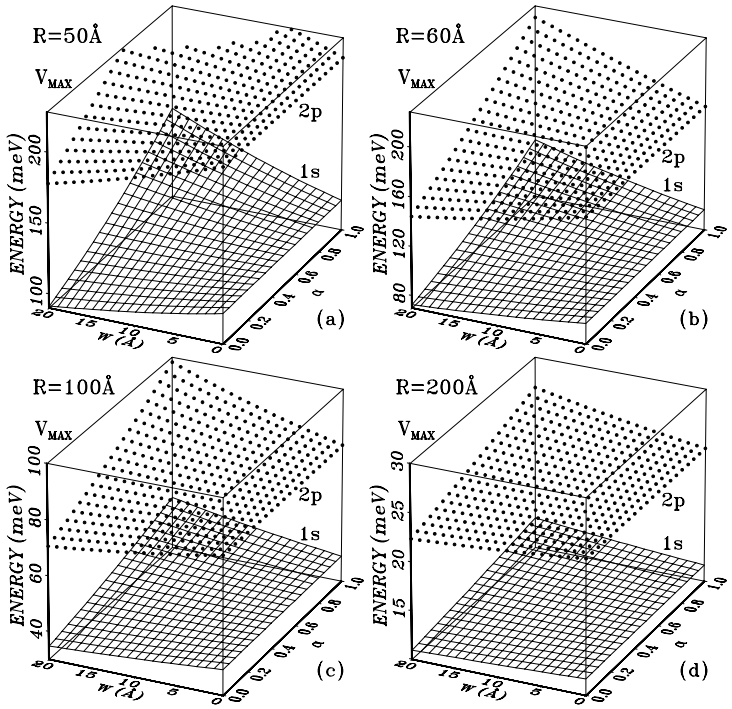

Fig. 3. Energy levels of the electron $1s$ (line-nets) and $2p$ (bullets) states as a function of the W and α interface parameters for four QDs with radii: (a) $R = 50$ Å, (b) $R = 60$ Å, (c) $R = 100$ Å, and (d) $R = 200$ Å.

will become wider too since the structure is moving from a QD to bulk $Al_{0.3}Ga_{0.7}As$ due to the finitely-high barrier. On the other hand, the effective mass approximation can be broken down if the height of the confinement potential is enhanced, *e.g.,* for the case of small quantum dots with an infinitely-high barrier.

The calculated electron energy levels of the confined $1s$ (nets) and $2p$ (bullets) states are plotted in Figure 3 in the $W - \alpha$ space for QDs with radii (a) $R = 50$ Å, (b) 60 Å, (c) 100 Å, and (d) 200 Å. Notice that the case $W = 0$ Å corresponds to dots having an abrupt interface, which can be taken as a reference to show the interface-fluctuation effects. The QD confinement influence on the electron changes from state to state (see Fig. 2). All the electron states will become degenerate with zero state energy when the dot size goes to infinite. That is not the case for a hydrogen atom where the degenerate states are dependent on their principal quantum numbers and the electron is always around the hydrogen ion. Due to the QD confinement, one of the electron states is confined more strongly, becoming the ground state, while the energy difference between the states increases for stronger confinement, which can be seen by comparing the cases for the different QD radii in Figure 3. The interface effect on the excited ($2p$) state is stronger than on the ground ($1s$) state. This is due to the fact that the electron in the $2p$ state has a larger average radius so that it is closer and more sensitive to the interface than the electron in the $1s$ state. When the interface is localized inside the dot ($\alpha = 1$), which corresponds to a stronger confinement dot due to the size-fluctuation, it blue shifts the electron energy levels. This blue-shift effect decreases when the interface moves further away from the dot center, and then a red shift comes out after a turning point. The interface influence on the energy levels becomes weaker with increasing dot size. It is obvious that the strongest interface effect on the $1s$ state occurs for the $R = 50$ Å dot, but it is also important in the $2p$ state case for the $R = 60$ Å dot because of the state spreading. The minimum dot radius for the $1s$ ($2p$) state to be bound is 24.8 (49.6) Å for the abrupt $GaAs/Al_{0.3}Ga_{0.7}As$ dot. Thus, the ground ($1s$) state can still be recognized as occurring in a strong confinement system like a $R = 50$ (60) Å $GaAs/Al_{0.3}Ga_{0.7}As$ dot, while the $2p$ state in a $R = 50$ Å dot is very close to a critical point at which there is a transition from a 0D to a 3D structure behavior.

Since the state energy levels shifts due to the interface effect can give an important contribution to the PL-spectrum broadening in QD samples [19], we show more clearly in Figure 4 the interface dependence of the energy levels of the two lowest states of an electron in an $R = 50$ Å dot. The energies of the $1s$ state and of the $2p$ state in the upper and lower panels of Figure 4, respectively, are depicted in the $W - \alpha$ space as isoenergetic lines (in meV units). Each associated energy value is relative to the corresponding levels in the abrupt dots. It is important to notice that:

(i) the energy shifts due to all the possible size fluctuations of QDs are separated into two different sectors, the blue-shift sector and the red-shift sector, by a boundary (solid curves with a zero value) in which the electron energies in

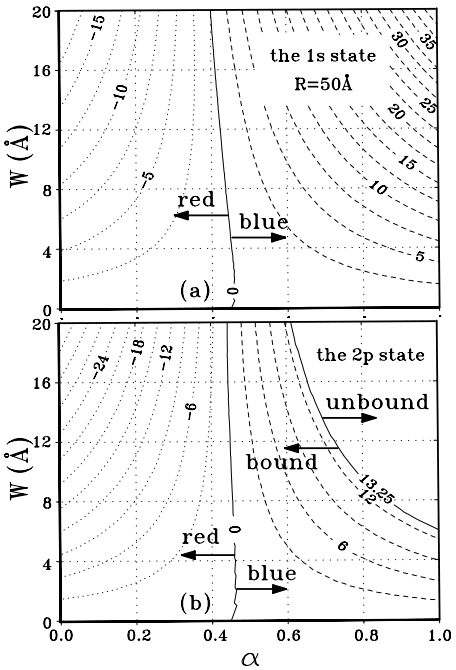

Fig. 4. $W - \alpha$ diagram for the $1s$ (a) and $2p$ (b) states of a free electron in a $R = 50$ Å $GaAs/Al_{0.3}Ga_{0.7}As$ quantum dot. The numbers in the isoenergetic lines indicate the state energy (in meV units) which is relative to those of a similar abrupt dot structure.

the graded QDs are equal to that in the sharp interface QD ($W = 0$);

(ii) the $2p$ state (see the lower figure) has a so called free state sector (unbound state $E_{2p} > V_{\rm MAX}$) in the strong confinement region (large α and wide W). With decreasing interface width and moving the interface close to the dot center, this state changes from unbounded to bounded when $E_{2p} < V_{\rm MAX}$, being the transition line displayed as a solid curve indicated by the value 13.25 meV;

(iii) the maximum energy difference of the intersubband ($1s \rightarrow 2p$) transition due to changes on the interface width for a set of single QD structures can be as large as 90 meV, and the broadening of this transition should be of the same order. Therefore, graded interface effects can contribute significantly to the intersubband transition energy broadening in QDs, and this contribution should be detectable through optical measurements;

(iv) a graded interface having a width from one to three GaAs lattice constants [20] in the $R = 50$ Å dot can turn the $2p$ state into an unbound one, if the part of the interface inside the dot is more than 60%. In this case, there are no bound excited states in the system anymore. This interesting result can explain qualitatively the recent experimental observation of the existence of only one PL peak from a single quantum dot published by two groups [18,19].

Since possible experimental results for the structures studied here may concern the intersubband transitions between two electron states, we display in Figure 5 the transition energy between the ground state ($1s$) and the lowest excited ($2p$) state of an electron in the $W - \alpha$ space for the same structures as shown in Figure 3. The reference planes indicated by the line nets characterize the $1s \rightarrow 2p$ transition energy for an electron in the corresponding structures with abrupt interfaces. The transition energy is smaller when the dot size increases since the carrier confinement becomes weaker, while it decreases when $R \rightarrow 0$ (see Fig. 5a for large α) since the bound $2p$ state is going to be a bulk $Al_{0.3}Ga_{0.7}As$ state, as discussed before. When compared to the shifts of the state-energy levels (see Fig. 3), the intersubband transition-energy shifts are relatively small because of the energy-shift cancellation of the ground state and the excited state. There are two opposite transition-energy shifts due to the interface effect, *i.e.*, the blue-shift (dots with a line above the reference plane) and the red-shift (dots with a line below the reference plane), which are separated by the dots without any tails in Figure 5. There is an additional remark for the $R = 50$ Å dot in the region of large α and wide W: the $2p$ state is no longer bound, which is represented by the existence of an empty sector in Figure 5a.

Although the size-fluctuation effect on the intersubband transitions is relatively weak as compared to the effect on the state energy levels, the transition-energy shifts due to this effect has been shown still to be significant in the strong confinement case. As can be seen from Figure 5, the transition from blue to red in the $R = 50$ Å dot occurs around $\alpha = 0.5$, and is weakly dependent on the interface width. With increasing dot radius, this transition will take place later. For instance, the values of α for the transition are 0.39, 0.40, 0.42, and 0.6 for the dots having a fixed interface width of $W = 20$ Å and radii $R = 200$ Å, 100 Å, 60 Å, and 50 Å, respectively. A faster increase in α occurs from $R = 60$ Å to $R = 50$ Å due to the fact that now the $2p$ state is moving into the unbound phase so that the interface-width effect becomes weaker, and consequently it needs a bigger α to compensate. There exists a three-sector intersection point for the blue-, red-shift and unbound sectors around $W = 20$ Å and $\alpha = 0.6$ for the $R = 50$ Å dot, while it is not the case for the $2p$ state energy as shown in Figure 4 because the blue shifts of both $1s$ and $2p$ states cancel each other. Away from the transition boundary consisting of the solid dots without lines, the shift of the $1s \rightarrow 2p$ transition energy due to the interface effect is considerably large, *e.g.*, an interface width $W = 10$ (20) Å inside (outside) the $R = 100$ Å dot enhances (decreases) the transition energy as much as about 5 (10) (3 (4)) meV. Such large difference for a single electron transition should be measurable by optical experiments.

4 The shallow donor states

By using the variational approach described in Section 2, a numerical calculation has been performed to obtain the energy levels and the wave functions of a shallow donor in a graded spherical $GaAs/Al_xGa_{1-x}As$ quantum dot,

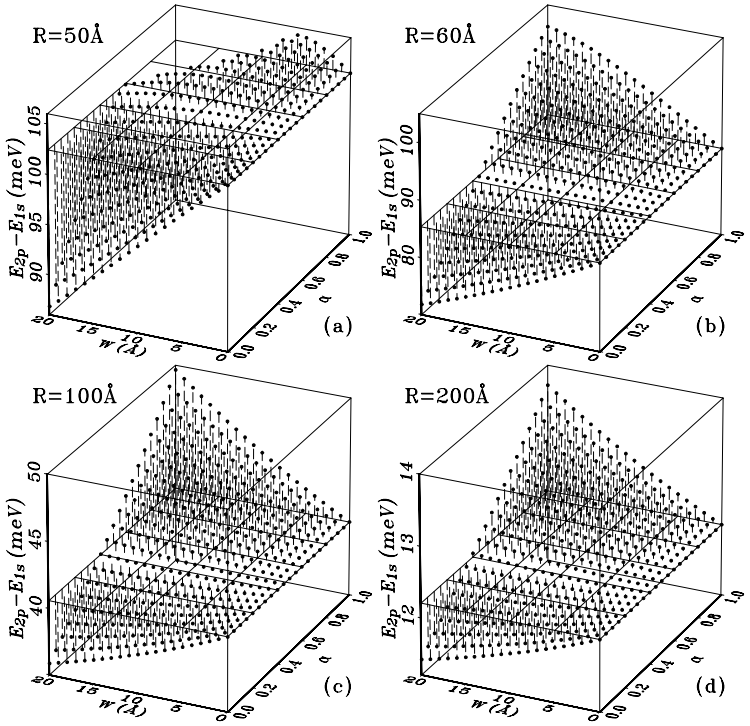

Fig. 5. $1s \rightarrow 2p$ transition energies (bullets) as a function of the W and α interface parameters for four QDs with radii: (a) $R = 50$ Å, (b) $R = 60$ Å, (c) $R = 100$ Å, and (d) $R = 200$ Å. Lines below and above the dots indicate the blue and red shifts, respectively. The empty area is the unbound $2p$ sector.

which may be located at any position inside the Gas region. There are two variational parameters in the trial wave function, as introduced in equation (9): one (β) describes the Coulomb interaction between the electron and the donor ion, and the other (γ) is related to the broken spherical symmetry of the system which occurs for the off-dot-center donor. Notice that the parameter β has the dimension of the reverse of length, while γ is dimensionless. Three facts [24] are helpful here for checking the numerical results: in the shallow donor absence, β is equal to zero since no Coulomb interaction is considered; in the presence of a dot-center donor, γ is always equal to one because of the spherical symmetry of the structure; finally, when the dot size becomes infinite and the donor is far away from the interface, both β (in units of $1/a_0^*$) and γ approach one to recover the hydrogenic atom-like behavior.

In order to understand the donor state [24], we have initially calculated three Ψ_{1s}-based state widths for a QD with abrupt interface ($W = 0$) as a function of the dot radius for a donor located at the dot center $R_0 = 0$ (solid), at the midpoint $R_0 = R/2$ (dashed) between the dot center and the interface, and in the interface $R_0 = R$ (dot-dashed curves). The state width $\langle\Psi_{1s}|(x^2 + y^2)/2|\Psi_{1s}\rangle^{1/2}$ in the x-y plane is plotted in Figure 6a, the state width $\langle\Psi_{1s}|z^2|\Psi_{1s}\rangle^{1/2}$ related to the dot center in the z direction is presented in Figure 6b, and the state width $\langle\Psi_{1s}|(z - R_0)^2|\Psi_{1s}\rangle^{1/2}$ for the donor center is depicted in Figure 6c.

We have found that the existence of a shallow donor allows the lowest bound state to occur even when

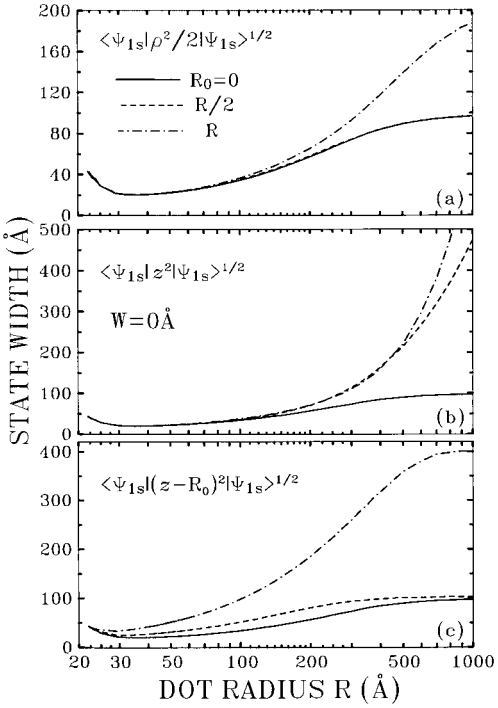

Fig. 6. The dot radius dependence of abrupt $GaAs/Al_{0.3}Ga_{0.7}As$ quantum dots of several state widths: (a) the state width $\langle\Psi_{1s}|(x^2 + y^2)/2|\Psi_{1s}\rangle^{1/2}$ in the x-y plane; (b) the state width $\langle\Psi_{1s}|z^2|\Psi_{1s}\rangle^{1/2}$ related to the dot center in the z direction; and (c) the state width $\langle\Psi_{1s}|(z - R_0)^2|\Psi_{1s}\rangle^{1/2}$ for the donor center. Three donor positions are considered: a dot-center donor (solid), a midpoint donor (dashed), and an interface donor (dot-dashed).

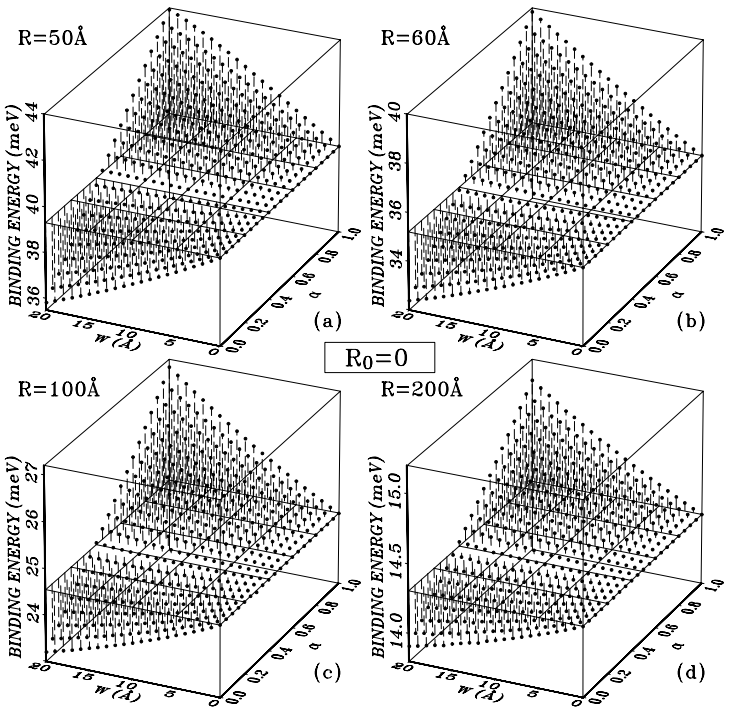

Fig. 7. Binding energy of a shallow donor at the dot center $R_0 = 0$ (bullets) as a function of the W and α interface parameters for four QDs with radii: (a) $R = 50$ Å, (b) $R = 60$ Å, (c) $R = 100$ Å, and (d) $R = 200$ Å. Lines below and above the dots indicate the relationship of the binding energy value with the blue and red interface related energy level shifts, respectively.

$R = R_{\rm MIN} = 22$ Å, which is smaller then the value obtained for a bound electron in an undoped dot (24.8 Å). This is due to the fact that the electron in the doped QD has a heavier average effective mass than in the undoped QD. The strongest QD confinement due to the shallow donor occurs when the dot radii is in the 30 - 40 Å range, where all the state widths are close to 20 Å, proving that the standard effective mass approximation description of a QD with a shallow donor is valid [26].

All the state widths and their differences decrease when the dot radius is reduced up to 30 Å since the Coulomb potential is much weaker than the 3D confinement potential. This also explains why the state width of a shallow donor in small doped QDs is very close to that of an electron in small undoped QDs, which can be seen by comparing Figure 6 with Figure 2. However, when R approaches the limit $R_{\rm MIN} = 22$ Å, the state widths become larger because the QD structure is turning to be bulk $Al_xGa_{1-x}As$. It is important to notice that:

(i) for a dot-center donor, the state width in the x-y plane is equal to one in the z direction (compare the three solid curves in Figure 6a, 6b and 6c) because of the spherical symmetry of the system. All of them approach to 98.7 Å (the GaAs effective Bohr radius) when the dot radius goes to infinite, been retrieved the 3D hydrogenic atom-like behavior;

(ii) the midpoint-donor state widths (solid lines) in the $x-y$ plane (Fig. 6a) and the donor center $(z-R_0)^2$ state (Fig. 6c) have a similar behavior as those of the dot-center donor (Fig. 6b). The z^2 state width for the center donor ($R_0 = 0$) is close to the interface donor ($R \neq 0$) when the dot radii are smaller than 500 Å, after which the difference between them increases dramatically. The interface donor z^2 state widths does not show any pinning behavior. The reason for this is that the confinement potential is relatively weak as compared to the Coulomb interaction. Consequently, the electron is moving tightly with the donor center, thus the average distance between the electron and the dot center becomes larger;

(iii) the state widths of an interface donor in the z direction increases much faster than in the x-y plane when the dot radius is larger because the confinement potential of the dot forces the electron to be closer to the dot center (*i.e.*, further away from the donor center), so that the distance along the z direction between the electron and the donor center becomes larger.

When $R \to \infty$, the interface donor behaves as in a heterostructure, where it is no longer possible to recover the 3D situation due to the existence of a barrier repellent force. However, an equilibrium will be set up between the Coulomb interaction and the barrier potential when the dot size increases. In this case, the state width concerning the donor center $(z - R_0)^2$ shows a pinning behaviour. The pinning behavior begins to occur at about 400 Å, which is four times larger than the width of a 3D donor. According to the standard theory for the relation between the radii and energies of the 3D hydrogenic states,

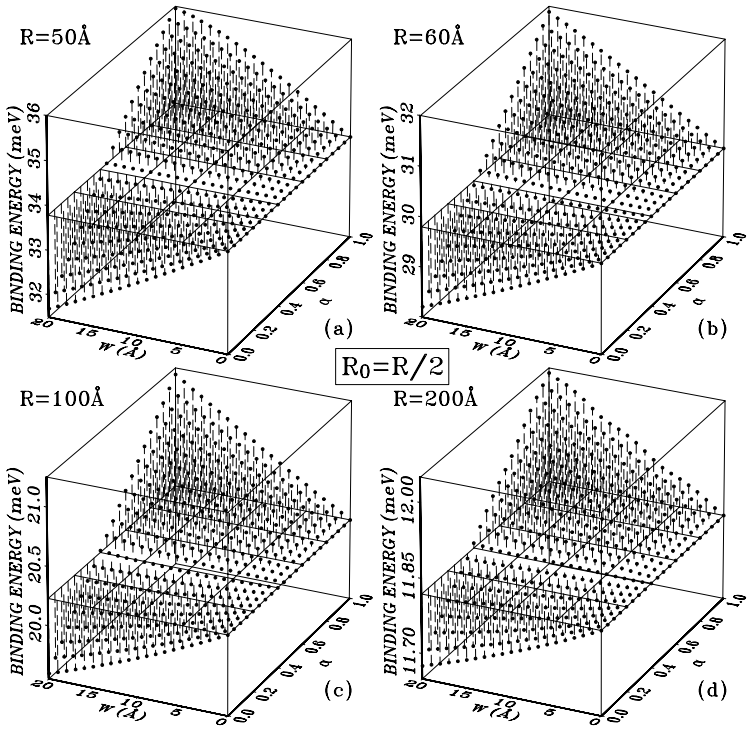

Fig. 8. Binding energy of a shallow donor at the dot center $R_0 = R/2$ (bullets) as a function of the W and α interface parameters for four QDs with radii: (a) $R = 50$ Å, (b) $R = 60$ Å, (c) $R = 100$ Å, and (d) $R = 200$ Å. Lines below and above the dots indicate the relationship of the binding energy value with the blue and red interface related energy level shifts, respectively.

we estimate the binding energy of the interface donor to be about four times smaller than one effective Rydberg, which is consistent with our numerical finding $0.23\,R^*$ in the limit $R \to \infty$. The state width in the x-y plane for the interface donor is pinned also but close to 180 Å, which is larger than one effective GaAs Bohr radius. This result is due to the fact that the dot barrier pushes the electron away from the interface where the donor is located. Thus, the electron is on average further away from the donor center than in a 3D donor case, and consequently the Coulomb interaction decreases, which in turn leads to an enhancement of the wave function extent in the x-y plane.

The binding energy of a shallow donor, which is an experimentally measurable quantity, can be obtained through equation (11). Before doing this, two calculations have to be performed: the first is the lowest energy level of a free electron in the QD with $Z_{\rm D} = 0$, and the second is the ground state of a shallow donor, which is associated with ψ_{1s} for $Z_{\rm D} = 1$. Figure 7 depicts the binding energy for the shallow donor at the dot center $R_0 = 0$ as a function of both the interface width W and the interface position α for $R = 50$ Å, 60 Å, 100 Å, and 200 Å. The stronger QD confinement forces the electron to be closer to the impurity center. As a consequence, the Coulomb interaction between the donor ion and the electron becomes stronger, which enhances considerably the shallow donor binding energy.

The interface effect is shown to be important only for strong confinement QDs. For instance, both the blue shift and the red shift of the binding energy are about 4 (2) meV when $R = 50$ Å ($R = 100$ Å) and 20 Å thick interfaces for $\alpha = 0$ or $\alpha = 1$ cases. Therefore, the binding energy shift for the small QDs due to the existence of the interface is also large enough to be detected by optical experiments. However, these shifts for a 200 Å dot are almost ten times smaller than those in the strong confinement QDs. It is clear from Figure 7 that the blue-shift and the red-shift sectors of the binding energy in the $W - \alpha$ space are separated by a transition line for α around 0.40∼0.45, where the energy shifts of the free electron state and the shallow donor state cancel each other. As compared to the transition energy of the electron in a undoped dot (see Fig. 5), the binding energy shift of the donor due to the interface fluctuation is smaller because the donor ion at $R_0 = 0$ attracts the electron so that the average state width spreading decreases, which leads the electron to be further away from the interface.

When the donor moves away from the dot center, the spherical symmetry of the system is broken. As a consequence, the electron wave function spreading is enhanced and the binding energy of the donor electron decreases. We see this behavior in Figure 8 and Figure 9 for a midpoint ($R_0 = R/2$) donor and an interface ($R_0 = R$) donor, respectively. Although the binding energy in the $W - \alpha$ space for the midpoint donor behaves similarly to that of a dot-center donor, it is about a quarter smaller,

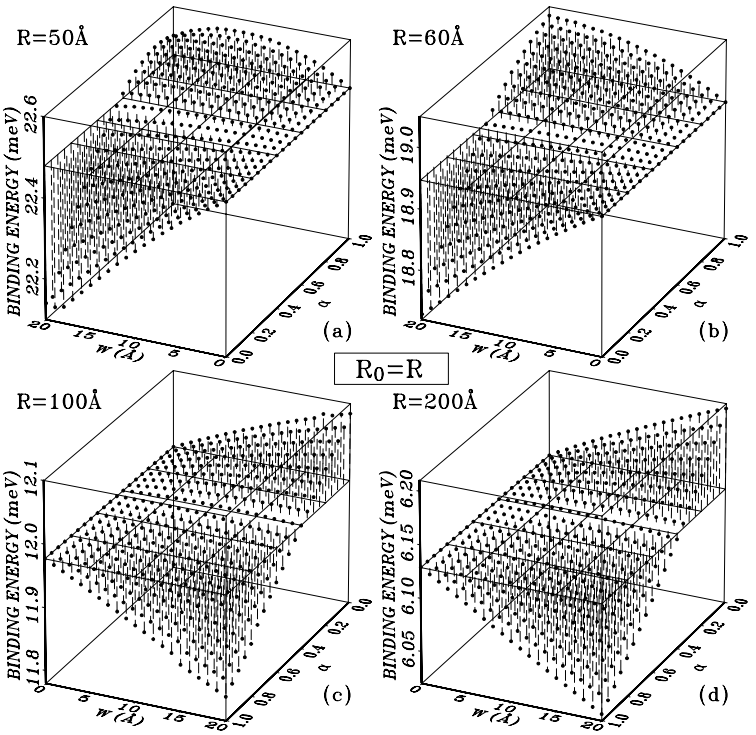

Fig. 9. Binding energy of a shallow donor at the dot center $R_0 = R$ (bullets) as a function of the W and α interface parameters for four QDs with radii: (a) $R = 50$ Å, (b) $R = 60$ Å, (c) $R = 100$ Å, and (d) $R = 200$ Å. Lines below and above the dots indicate the relationship of the binding energy value with the blue and red interface related energy level shifts, respectively.

and its shift due to the interface fluctuation is about a half less for the small dots ($R = 50$ Å, and 60 Å), and about three fourths less for the larger dots ($R = 100$ Å, and 200 Å). In fact, the interface effect can be neglected for the $R = 200$ Å dot since it provides a maximum blue (red) shift of only 0.22 (0.14) meV, which is comparable with the typical accuracy of 2 cm^{-1} ($\sim$0.25 meV) attained in recent optical experiments [2].

The state widths of the interface donor have a different character from those of the dot-center and midpoint donors for the larger QDs. All the shifts of the shallow donor binding energy in large QDs due to graded interfaces are experimentally negligible due to their small absolute values. For the strong confinement dot $R = 50$ Å with $\alpha \to 1$, the binding energy does not grow monotonously when the interface width increases as it does for the dot-center and midpoint donor. The reason for this is of two fold: first, the interface donor has a higher energy than the others, which forces the asymptotic 3D behavior earlier in the strong confinement QDs; and second, the Coulomb potential is screened by the barrier when $\alpha \to 1$ and $W \neq 0$, so that such dressed potential is weaker for the electron binding. The blue-shift and the red-shift sector in Figure 9 exchange their position in the $W - \alpha$ space when the dot radius increase - compare Figure 9a and Figure 9b to Figure 9c and Figure 9d. This can be understood qualitatively by the following. For the large dots, the influence of a dot-size fluctuation on the electron energy can be very weak, while changing α in the case of a fix W is equivalent to such fluctuation. On the other hand, the screened Coulomb potential varies also, which may increase (decrease) the binding energy of the donor when it moves out of (into) the $Al_xGa_{1-x}As$ alloy region.

Finally, we show in Figure 10 the dot-radius dependence of the binding energy for a shallow donor which is located at three typical positions: $R_0 = 0$ (upper-), $R_0 = R/2$ (middle-), and $R_0 = R$ (lower-group curves) in a graded QD. The QD interface is supposed to be at three typical positions indicated by (a) $\alpha = 0.0$, (b) $\alpha = 0.5$, and (c) $\alpha = 1.0$ and having three different widths $W = 0$ Å (solid), $W = 10$ Å (dashed), and $W = 20$ Å (dot-dashed curves). It is clearly shown in Figure 10(b) that the interface effect on the binding energy is small, despite the important interface related correction on the QDs energy levels. An effective method to diminish the energy broadening in a QD structure is through a shallow donor doping in the interface, which can be observed from Figure 10. Comparing Figure 10a with Figure 10c, we can see when $\alpha = 0$ that a wider interface decreases the QD confinement, while when $\alpha = 1$ a wider interface enhances the QD confinement. If the dot is large enough, the states of the dot-center ($R_0 = 0$) and of the midpoint ($R_0 = R/2$) donors degenerate, presenting an asymptotic behavior as a donor in bulk GaAs. On the other hand, the interface ($R_0 = R$) donor is always in contact with two different semiconductors, so that the potential of the barrier pushes the electron away from the donor center, resulting that its

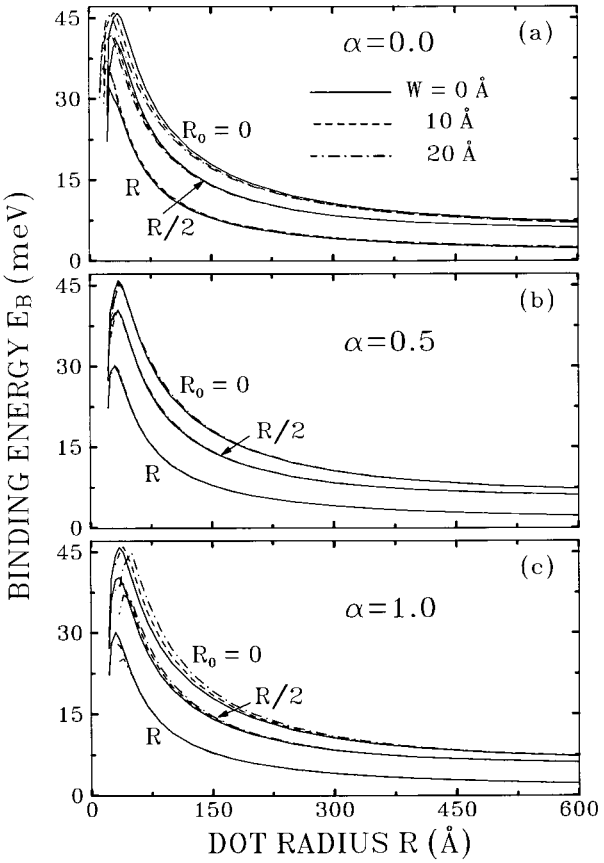

Fig. 10. Dot-radius dependence of the binding energy of a donor at three typical positions: $R_0 = 0$ (upper group of curves), $R_0 = R/2$ (middle group of curves) and $R_0 = R$ (lower group of curves) in graded GaAs/$Al_{0.3}Ga_{0.7}$As quantum dots with interfaces widths $W = 0$ Å (solid), $W = 10$ Å (dashed), and $W = 20$ Å (dotted dashed curves), and locations (a) $\alpha = 0.0$, (b) $\alpha = 0.5$, and (c) $\alpha = 1.0$.

binding energy is dependent on the barrier height, weakly than that of a donor in bulk materials.

In the present case ($x = 0.3$), we found that the binding energy of the interface donor in the abrupt dots approaches to $0.23\,R^*$. When the dot radius decreases, the binding energy of the donor state first increases, and reaches the maximum value around $R = 35$ Å (see Fig. 6), decreasing when $R \to 0$. This behavior is due to the finite height of the $Al_xGa_{1-x}As$ barrier, which makes the system behavior to change from 3D GaAs to a GaAs/Al_xGa_{1-x}As QD, and finally to bulk $Al_xGa_{1-x}As$. The maximum binding energy (∼45 meV) of a shallow donor in the GaAs/$Al_{0.3}Ga_{0.7}$As QDs is about 1.5, 3 and 9 times higher than the binding energies in quantum wires, QWs, and in bulk GaAs, that are 30 meV, 15 meV and 6 meV, respectively [5,34]. As a consequence of the dot-size fluctuation related to the width and/or the position of the interface, the actual value of $R_{\rm MIN}$ changes. For instance, when the interface width $W = 10$ (20) Å and $\alpha = 1.0$ (0.5; 0.0), the minimum dot radius for the possible bound ground state is 18 (13) (23 (23); 28 (33)) Å.

5 Conclusions

We have performed a theoretical study on the interface related energy level shifts of electrons in graded GaAs/Al_xGa_{1-x}As QDs, without and with the presence of a shallow donor. The interface description was based on the assumption that a graded $Al_{y(r)}Ga_{1-y(r)}As$ alloy exist in the interface region between GaAs and $Al_xGa_{1-x}As$. Considering a linear variation for the interfacial Al profile, we have obtained expressions for the QD confinement potential and electron effective mass in the interface region. A multistep potential scheme was developed to accurately solve Schrödinger-like equations to obtain the wave functions and the energy levels of the electron states. When shallow donors were considered, a variational approach was used to calculate the electron bound states. The graded interface effects were analyzed through two parameters, one associated to the interface width (W), and the other (α) describing the interface positioning. Isoenergetic lines in the $W - \alpha$ interface space were shown to be a convenient picture to describe the interface related energy level broadening.

The interface effect was found to produce a blue or a red shift on the energy levels of electrons and donors in GaAs/Al_xGa_{1-x}As QDs, and consequently a blue or red shift in their intersubband transition and donor binding energies. These shifts depend not only on the interface width, but also on the interface and on the donor position. In strong confinement systems, they are very large and should be observable in experiments. The interface effect was shown to be stronger in excited than in ground state energy level states. Shifts on the intersubband transition energies as large as 90 meV were obtained for the strong confinement case. It was shown that doping the graded interface region of quantum dots can reduce considerably the interface related shifts of their energy levels, as much as 20 meV in the strong confinement case (dots with ∼ 50 Å radius and a 20 Å wide interface).

Recent experimental work on the PL spectra obtained by probing just one single QD found only one PL peak, and an explanation of its position needed a smaller dot radius than actually it was estimated considering sharp interfaces [18,19]. This seems to support that the interface region is restricted to be completely inside the QD ($\alpha = 1$). However, a direct comparison of our results with experimental data are not possible since: (i) the interface of GaAs/Al_xGa_{1-x}As QDs were not characterized yet, to the knowledge of the authors; (ii) we have not considered holes and the electron-hole interaction in the Hamiltonian (1), and consequently it is not possible to calculate the exciton binding energy in the QDs. Our results highlight that an estimation of the dot radius to be used in a sharp interface model needs detailed information on the actual localization and width of the dot interface. Although the results presented in this work were obtained for a GaAs/$Al_{0.3}Ga_{0.7}$As spherical QD, they are also valid for QDs of other types of semiconductors, with changes in the figures of merit however. The approach developed here can be easily generalized for interfaces with different shapes, as well as for others low dimensional structures.

Further studies on the these possibilities and on the study of interface effects on the exciton binding energy (including also the presence of applied external electric and magnetic fields) are in progress within the $W - \alpha$ interface description scheme. Finally, the interface description can be easily used to investigate different types of interface profiles by changing the function $y(r)$ (see Eq. (3)). However, the main conclusions of the present work will not change.

One of us (J.M.S.) would like to acknowledge a visiting professor fellowship from the Science Funding Agency of the Ceará State in Brazil (FUNCAP). G.A.F. and V.N.F. would like to acknowledge the financial support received from FUNCAP, the Brazilian National Research Council (CNPq), and the Ministry of Planning (FINEP).

References

1. T. Ando, A.B. Fowler, F. Stern, Rev. Mod. Phys. **54**, 437 (1982).
2. J.P. Cheng, B.D. McCombe, J.M. Shi, F.M. Peeters, J.T. Devreese, Phys. Rev. B **48**, 7910 (1993).
3. J.M. Shi, F.M. Peeters, J.T. Devreese, Phys. Rev. B **50**, 15 182 (1994).
4. J.L. Zhu, J.J. Xiong, B.L. Gu, Phys. Rev. B **41**, 6001 (1990).
5. S.V. Branis, G. Li, K.K. Bajaj, Phys. Rev. B **47**, 1316 (1993).
6. D.S. Chuu, C.M. Hsiao, W.N. Mei, Phys. Rev. B **46**, 3898 (1992).
7. C. Sikorski, U. Merkt, Phys. Rev. Lett. **62**, 2164 (1989).
8. Y. Arakawa, H. Sasaki, Appl. Phys. Lett. **40**, 939 (1982).
9. D. Gammon, E.S. Snow, B.V. Shanabrook, D.S. Katzer, D. Park, Phys. Rev. Lett. **76**, 3005 (1996) and references therein.
10. R. Leon, P.M. Petroff, D. Leonard, S. Fafard, Science **267**, 1966 (1995).
11. K. Brunner, G. Abstreiter, G. Böhm, G. Tränkle, G. Weimann, Phys. Rev. Lett. **73**, 1138 (1994).
12. D. Gammon, E.S. Snow, D.S. Katzer, Appl. Phys. Lett. **67**, 2391 (1995).
13. See *e.g.*, D. Jovanovic, J.P. Leburton, Phys. Rev. B **50**, 5412 (1994).
14. A.A. Reeder, J.M. Mercy, B.D. McCombe, IEEE J. Quantum Electron. **QE-24**, 1690 (1988), and references therein.
15. U. Merkt, Physica B **189**, 165 (1993).
16. A.P. Alivisatos, Science **267**, 933 (1996).
17. D.J. Norris, M.G. Bawendi, Phys. Rev. B **53**, 16338 (1996).
18. Y. Nagamune, H. Watabe, M. Nishioka, Y. Arakawa, Appl. Phys. Lett. **67**, 3257 (1995).
19. S.A. Empedocles, D.J. Norris, M.G. Bawendi, Phys. Rev. Lett. **77**, 3873 (1996).
20. See *e.g.*, A. Ourmazd, D.W. Taylor, J. Cunningham, C.W. Tu, Phys. Rev. Lett. **62**, 933 (1989).
21. M.A. Herman, D. Bimberg, J. Christen, J. Appl. Phys. **70**, R1 (1991), and references therein.
22. J.L. Zhu, D.L. Lin, Y. Kawazoe, Phys. Rev. B **54**, 16 786 (1996).
23. V.N. Freire, J.M. Shi, G.A. Farias, in *Quantum Confinement IV: Nanoscale Materials, Devices, and Systems*, edited by M. Cahay, J.P. Le Burton, D.J. Lockwood, S. Bandyopadhyay (Electrochemical Society PV 97-11, Montreal, Canada, 1997).
24. J.M. Shi, V.N. Freire, G.A. Farias, in *Quantum Confinement IV: Nanoscale Materials, Devices, and Systems*, edited by M. Cahay, J.P. Le Burton, D.J. Lockwood, S. Bandyopadhyay (Electrochemical Society PV 97-11, Montreal, Canada, 1997).
25. O. Albrektsen, D.J. Arent, H.P. Meire, H.W.M. Salemink, Appl. Phys. Lett. **57**, 31 (1990).
26. W. Kohn, Solid State Phys. **5**, 257 (1957).
27. S. Adachi, J. Appl. Phys. **58**, R1 (1985).
28. V.N. Freire, M.M. Auto, G.A. Farias, Superlatt. Microstruct. **1**, 17 (1992); R. Renan, V.N. Freire, M.M. Auto, G.A. Farias, Phys. Rev. B **48**, 8446 (1993); M.C.A. Lima, G. A. Farias, V.N. Freire, Phys. Rev. B **52**, 5777 (1995); E. C. Ferreira, J. A. P. da Costa, G.A. Farias, V.N. Freire, Superlattices and Microstructures **17**, 397 (1995).
29. H.J. Lee, L.Y. Juravel, J.C. Wolley, A.J. Springthorpe, Phys. Rev. B **21**, 659 (1980).
30. See *e.g.,* J. Irving, N. Mullineux, *Mathematics in Physics and Engineering*, (Academic, New York, 1959) Sec. 6.2., p. 345.
31. Y. Ando, T. Itoh, J. Appl. Phys. **61**, 1497 (1987).
32. G. Bastard, Phys. Rev. B **24**, 4714 (1981).
33. R.L. Greene, Bajaj, Phys. Rev. B **31**, 913 (1985).
34. F.M. Peeters, J.M. Shi, J.T. Devreese, Physica Script. **T55**, 57 (1994).